scientific reports

Check for updates

OPEN

Repurposing the Pathogen Box compounds for identification of potent anti-malarials against blood stages of *Plasmodium falciparum* with PfUCHL3 inhibitory activity

Hina Bharti, Aakriti Singal, Manisha Saini, Pradeep Singh Cheema, Mohsin Raza, Suman Kundu & Alo Nag✉

Malaria has endured as a global epidemic since ages and its eradication poses an immense challenge due to the complex life cycle of the causative pathogen and its tolerance to a myriad of therapeutics. PfUCHL3, a member of the ubiquitin C-terminal hydrolase (UCH) family of deubiquitinases (DUBs) is cardinal for parasite survival and emerges as a promising therapeutic target. In this quest, we employed a combination of computational and experimental approaches to identify PfUCHL3 inhibitors as novel anti-malarials. The Pathogen Box library was screened against the crystal structure of PfUCHL3 (PDB ID: 2WE6) and its human ortholog (PDB ID: 1XD3). Fifty molecules with better comparative score, bioavailability and druglikeliness were subjected to in-vitro enzyme inhibition assay and among them only two compounds effectively inhibited PfUCHL3 activity at micro molar concentrations. Both MMV676603 and MMV688704 exhibited anti-plasmodial activity by altering the parasite phenotype at late stages of the asexual life cycle and inducing the accumulation of polyubiquitinated substrates. In addition, both the compounds were non-toxic and portrayed high selectivity window for the parasite over mammalian cells. This is the first comprehensive study to demonstrate the anti-malarial efficacy of PfUCHL3 inhibitors and opens new avenues to exploit UCH family of DUBs as a promising target for the development of next generation anti-malaria therapy.

Abbreviations

PfUCHL3	*Plasmodium falciparum* ubiquitin C-terminal hydrolase 3
DUB	Deubiquitinase
MMV	Medicine for malaria venture
MTT	3-(4,5-Dimethylthiazol-2-yl)-2,5-diphenyl tetrazolium bromide
HepG2	Human hepatocellular carcinoma
HEK-293T	Human embryonic kidney
Ub-AMC	Ubiquitin C-terminal 7-amido-4-methylcoumarin
IPTG	Isopropyl β-D-1-thiogalactopyranoside
PTM	Post translational modifications
IC_{50}	Half maximal inhibitory concentration
S.I.	Selective index

Malaria is a globally acknowledged parasitic disease that causes an enormous socio-economic burden worldwide. Despite endless preventive measures, it continues to impact millions of people across the regions of sub-Saharan Africa and Asia, impelling thousands of deaths annually[1]. It is caused by six species of the unicellular eukaryotic

Department of Biochemistry, University of Delhi South Campus, Benito Juarez Road, New Delhi 110021, India. ✉email: anag@south.du.ac.in

pathogen of the genus *Plasmodium* and is mainly transmitted by the bite of an infected female *Anopheles* mosquito. *P. falciparum* being the deadliest among all the malaria causing *Plasmodium* species and accounts for the highest mortality rate[2]. Presently, an orchestra of sensitive diagnostic tools, effective chemotherapeutics, and vector control strategies have contributed immensely to limit the prevalence of this disease[3–5]. Undoubtedly, Artemisinin-based combination therapy (ACT) is the most effective treatment for malaria and accounts for reduced mortality. However, a major setback in the treatment of this disease appears with the occurrence of Artemisinin resistant *Plasmodium* strain in Thailand–Cambodia borders[6,7]. The persistence of resistance against other partnered non-clinical drugs with associated toxicity, limits the responsiveness of these drugs during the treatment regimen[8–11]. Furthermore, Mosquirix, the only licensed first-generation RTS, S/AS01 vaccine exhibits limited protection with an efficacy rate of only thirty percent[12,13]. Altogether, the dearth of effective vaccines and potent drugs against malaria warrants an absolute urgency to identify novel therapeutics with distinctive mode of action and molecular targets.

Surprisingly, unlike other eukaryotes, *Plasmodium* species own few transcription regulators[14,15], thereby, ascertaining the functional relevance of post translational modification (PTM) modulators in the parasite life cycle. Amidst varied PTMs, ubiquitination is an evolutionarily conserved class of PTMs that serves versatile cellular purposes in different eukaryotic organisms, including *Plasmodium*[16]. The ubiquitous involvement of this cascade in nearly every cellular and biological process enables the parasite for an elaborated adaptation to the staggeringly variable cellular environment that the parasites encounter across their multistage life cycle[17,18]. Moreover, a major proportion of parasite proteome is identified as the potential target for ubiquitination, and these ubiquitin tagged substrate are detected across all the asexual stages of the parasite life cycle[16]. Several knockout and experimental inhibition studies have identified various members of this pathway to be of clinical significance[19–21]. Owing to such essential character, the craftsmen of this pathway represent an attractive drug target for the development of newer antimalarials. Ubiquitin modification is carried out by sequential interplay of three enzymes namely E1, E2, and E3, whereas, the process is reversed by a highly specialized family of enzymes known as deubiquitinases (DUBs)[22]. DUBs are a group of proteases that removes the ubiquitin moiety from substrates by cleaving isopeptide linkages at the C-terminus of ubiquitin and regulates a plethora of cellular processes such as ubiquitin homeostasis, apoptosis, cell cycle progression, stress response, cell signalling and DNA damage, among others[23–27]. Any aberration in DUBs regulated pathways is associated with severe implications in various diseases such as cancer, inflammatory and neurodegenerative diseases[28–31]. Not surprisingly, DUBs are even identified as the key modulators of unicellular parasitic protozoans, therefore, they may serve as an attractive therapeutic target in several infectious diseases[32–35]. Likewise, several proteasome inhibitors such as Salinosporamide[36], Bortezomib[37], Epoxomicin[38] and MLN-273[39] have been shown to inhibit the growth and development of the malarial parasite. Moreover, resistance to Artemisinin is linked with the missense mutation in a gene encoding a deubiquitinase (UBP-1) on chromosome 2 in *P. chabaudi* Artemisinin resistant strain AS-ATN[40–42]. Together, these studies render DUBs as promising candidates for targeted therapeutic development against malaria.

Plasmodium falciparum encodes well-defined deubiquitination machinery with 29 DUBs and DUB-like proteins[43], classified as cysteine protease [ubiquitin-specific processing proteases (USP/UBP), ovarian tumor domain-containing proteases (OTU), Machado-Josephin domain (MJD) DUBs, ubiquitin C-terminal hydrolases (UCH)] and zinc-metalloprotease [JAMM/MPN motif proteases (JAMM)][44]. Among these, members of the cysteine protease family of DUBs have been identified as crucial mediators of the parasite life cycle. For instance, inhibition of PfUSP14 results in parasite death by altering the cellular ubiquitin homeostasis[45]. Whereas, PfOTU maintains parasite apicoplast by associating with Atg8[35]. Overexpression of a functional mutant of PfUCHL3 exerts a dominant-negative effect on wild type parasites, thereby, highlighting its inevitable role in parasite survival[46]. Among known DUBs in *P. falciparum*, UCHL3 is a structurally characterized deubiquitinase exhibiting dual activity and is a validated drug target. Whereas, in eukaryotes, UCHL3 is known to regulate numerous cellular pathways including oocyte maturation[47], DNA damage sensing and repair[48,49] and stress management[50]. Recently, it has emerged as an anti-cancer[51–53] and anti-neurodegenerative[54] therapeutic target as well. Surprisingly, despite the evolutionarily conserved biochemical traits, PfUCHL3 exhibits modest similarity to *Homo sapiens* UCHL3 (HsUCHL3) and displays considerable architectural variation in residues defining interaction in the active site pocket[55]. In comparison to human ortholog, the residues lining the binding groove of PfUCHL3 exhibits notable differences, which facilitate the formation of completely distinct interactions with its substrate. These interactions aid PfUCHL3 to attain a different conformation from its mammalian ortholog. Notably, the catalytic triad of PfUCHL3 lies within the milieu of functional interaction and undergoes minor conformational changes upon substrate binding as compared to HsUCHL3 whose active site is occluded by loop and undergo major changes upon substrate binding[46]. Hence, such differential structural characteristics can be exploited for the identification of pathogen selective inhibitors. Several studies employing structure based drug design approach have been reported for the identification of potent yet selective anti-malarials[56–58]. In this pursuit, we hypothesized that inhibitors targeting PfUCHL3 will possibly act as potent therapeutics in malaria therapy. However, developing a novel pharmacological agent is a time-consuming, extremely costly and high-risk process[59]. On the contrary, drug repurposing is a powerful alternative approach to overcome the above challenges[60].

Drug repurposing (even known as repositioning, reprofiling or re-tasking) is a process for identification of new therapeutic potential of an existing drug (approved/investigated against different diseases)[61]. With this aim, Medicines of Malaria Ventures (MMV) assembled and released Pathogen Box in 2015, consisting of 400 pure compounds active against Type II and III diseases[62]. Based on their activity, these compounds are grouped into varied pathogen specific categories[63]. Several studies have repurposed the Pathogen Box compounds against an array of diseases to identify novel inhibitors that provide a rudimentary scaffold as a primitive tool for drug discovery[62–67]. Therefore, these studies intrigued us to repurpose MMV Pathogen Box compounds for the identification of novel PfUCHL3 inhibitors that may act as potent anti-malarials.

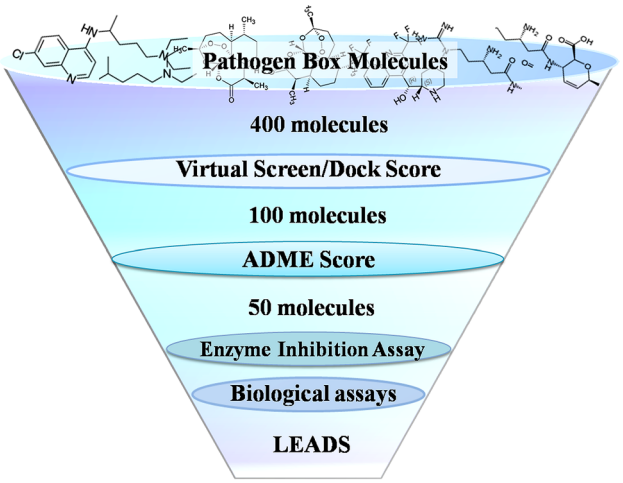

Figure 1. Schematic representation of the methodology for identification of potent hits against PfUCHL3: a flowchart illustrating the series of in-silico and in-vitro protocols employed to identify potent hits.

In this study, we employed structure-based drug discovery approach to repurpose 400 compounds from MMV Pathogen Box as novel anti-malarial with PfUCHL3 inhibitory effect. Herein, we docked Pathogen Box compounds against a grid encompassing active site residues and neighboring residues of PfUCHL3 and HsUCHL3. Based on comparative dock score and ADME (absorption, distribution, metabolism and excretion) profiling, best fifty candidates were assessed against in-vitro activity of *P. falciparum* UCHL3. Further, in-silico approaches were employed to gain insight into the enzyme-inhibitor interactions and the efficacy of the most promising hits was evaluated against the blood stages of *P. falciparum* in culture. The selectivity of lead compounds for parasites over the mammalian cell lines was also assessed. We present the first report attempting to identify the novel inhibitors targeting PfUCHL3 with potent inhibition of parasite growth. In the process, this study provides new chemical scaffolds that may serve as a template to develop more specific and potent clinical therapeutics against malaria.

Results

Structure based virtual screening (SBVS). SBVS approach was employed to identify novel anti-PfUCHL3 molecules. A flow chart depicting the screening methodology is illustrated in Fig. 1. Molecular docking algorithms were used to screen 400 compounds against the X-ray crystallographic structure of the enzyme (PDB ID: 2WE6) and with its human correspondent (PDB ID: 1XDT), which shares only 30% identity. Each molecule was docked 50 times in different conformations at the active site cleft of both the enzymes and the top hundred molecules were picked on the basis of higher selectivity towards *P. falciparum* UCHL3 than its mammalian counterpart (Table S1).

Next, the compounds exhibiting drug like properties, i.e. with acceptable range of pharmaceutically relevant properties and with zero violation of Lipinski rule of five were selected. Pharmaceutically relevant properties such as the partition coefficient (log Po/w) critical for estimation of absorption of drugs within the body, log Kp predicting skin permeability and log S exhibiting water solubility of the compounds were assessed, and eventually Pan-assay interference compounds which give false positive biological output were rejected[68]. As presented in Table S2, among the set of hundred compounds, based on SWISSDOCK-based ADME predictions, fifty distinct chemical entities that entirely fit inside the pink zone region of the bioavailability radar that displays the rapid appraisal of drug likeliness, were further investigated for their activity on recombinant PfUCHL3 in vitro.

Expression, purification and in-vitro assessment of compounds for enzyme inhibition. *Plasmodium falciparum* and human UCHL3 were expressed and purified to homogeneity as a single band around 30 kDa on SDS-PAGE (Fig. 2a–e). Both the enzymes were found to be catalytically active as evaluated by deubiquitinase assay (Fig. 2f). Subsequently, we evaluated the performance of the potential fifty compounds identified from *in-silico* studies against the catalytically active enzyme at a concentration of 100 µM with NEM (a known inhibitor of cysteine protease) as a positive internal control. At this concentration, the majority of compounds were ineffective on PfUCHL3 activity, whereas, four compounds showed more than thirty percent inhibition and only two of them (MMV676603 and MMV688704) exhibited an inhibition rate of more than fifty percent, as shown in Fig. 3.

Compounds with more than 50% enzyme inhibition were further evaluated for their inhibitory potential in a dose-dependent manner. As shown in Fig. 4a,b, compounds MMV676603and MMV688704 displayed an IC_{50} value of 25.12 ± 1.80 µM and 87.14 ± 1.75 µM, respectively. Concomitantly, due to the limited availability of the compounds, we evaluated these compounds only at their respective IC_{50} values against closely related human ortholog and observed no discernable effect on HsUCHL3 activity. The findings allude to the fact that both MMV676603 and MMV688704 hold the potential to inhibit in-vitro activity of PfUCHL3 over its mammalian ortholog with MMV676603 being a more potent inhibitor.

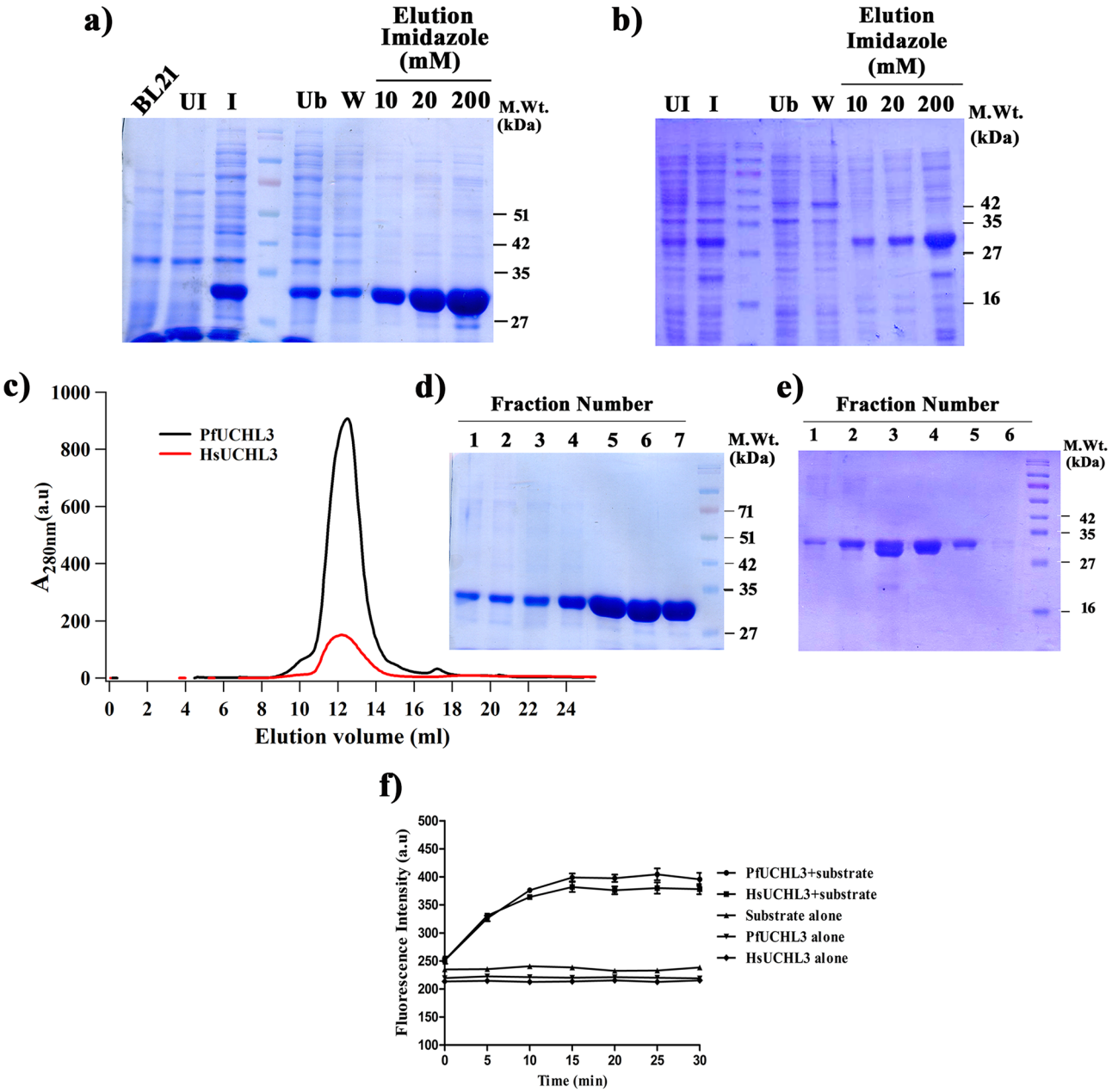

Figure 2. Expression, purification and deubiquitinating activity of PfUCHL3 and HsUCHL3: (**a**) PfUCHL3 and (**b**) HsUCHL3 were expressed in BL21 (λDE3) and purified using Ni-affinity chromatography, UI-uninduced, I-induced, Ub-unbound, W-wash. The proteins were further purified by gel filtration chromatography using AKTA prime. (**c**) The FPLC profile denotes a single peak for both the enzymes. Both (**d**) PfUCHL3 and (**e**) HsUCHL3 were purified to homogeneity as determined by SDS-PAGE analysis. (**f**) The catalytic activities of both the enzymes were assessed by measuring the change in fluorescence intensity, substrate and enzyme alone were taken as negative control. Uncropped images of commassie stained SDS gels are provided in Supplementary Fig. S1.

Molecular docking analysis of the lead compounds. Molecular docking provides the best-fit pose of the ligand in the protein structure that allows the explicit analysis of protein–ligand interactions. Accordingly, compounds MMV676603 and MMV688704 showed the binding energies of − 7.23 and − 6.15 kcal/mol, respectively for PfUCHL3. In contrary, both MMV676603 and MMV688704 lack specific binding to human UCHL3 and displayed the binding energies of 0.18 and − 1.6 kcal/mol respectively (Table 1). Docking analysis provides the predicted IC_{50} values for MMV676603 and MMV688704 against PfUCHL3 as 4.99 and 30.91 μM, respectively. In sharp contrast, the predicted IC_{50} value for MMV676603 against HsUCHL3 was not defined because of its positive binding energy value, for e.g. 0.8, however, for MMV688704, it was found to be 67.09 mM, as summarized in Table 1. Together, these results imply that compounds MMV676603 and MMV688704 harness more specific inhibitory action on PfUCHL3 than its mammalian ortholog.

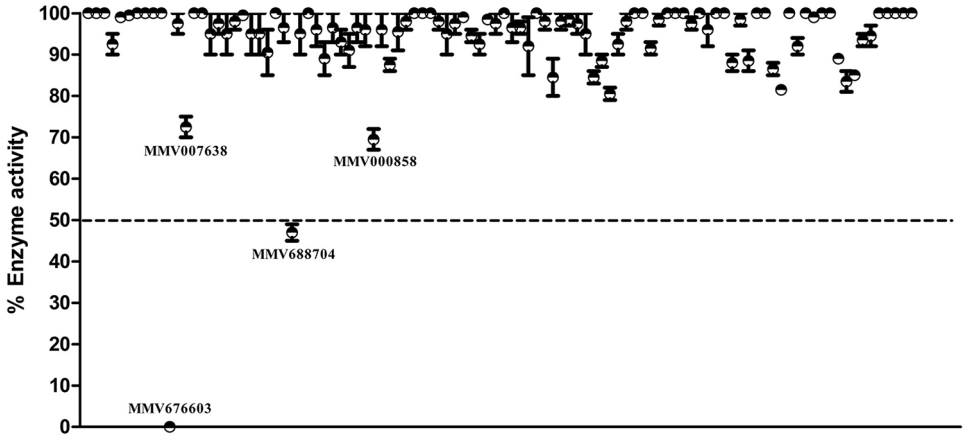

Figure 3. In-vitro screening of best hundred hits against PfUCHL3 activity: a scatter plot representing percent enzyme activity inhibition of fifty promising Pathogen Box compounds, identified from computational evaluation at 100 μM concentration. The dashed line at 50 is considered as inhibitory cutoff. Compounds with more than 50% inhibition threshold were considered for further screening. Bar denotes the standard deviation (n = 3) for each compound.

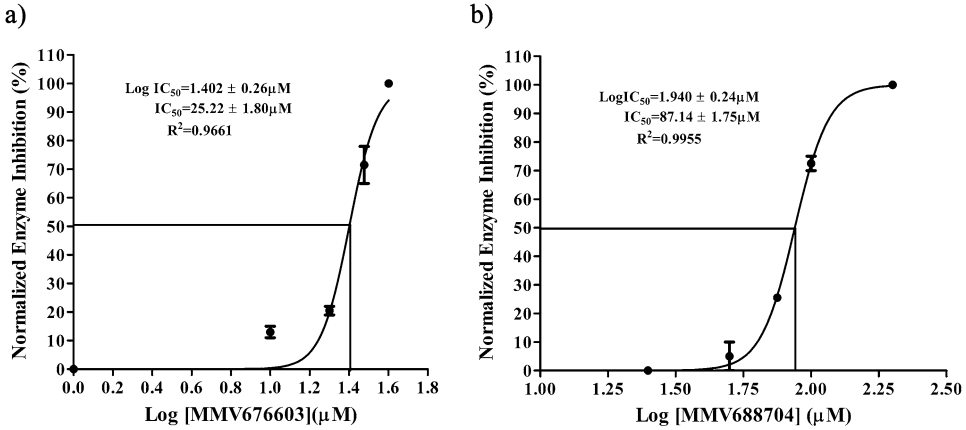

Figure 4. IC_{50} determination of the compounds MMV676603 and MMV688704 against PfUCHL3 activity: dose–response curve indicating the Log IC_{50}, IC_{50} and R^2 values of (**a**) MMV676603 and (**b**) MMV688704 against recombinant PfUCHL3. Inhibition at each data point is depicted as Mean ± S.D. of three independent experiments.

Name of the compound	△G (kcal/mol) against PfUCHL3 (PDB ID:2WE6)	△G (kcal/mol) against HsUCHL3 (PDB ID:1XD3)	Comparative △G (kcal/mol)	Predicted IC_{50} value against PfUCHL3 (μM)	Predicted IC_{50} values against HsUCHL3
MMV676603	− 7.23	0.18	− 7.41	4.99	N.D
MMV688704	− 6.15	− 1.6	4.55	30.91	67.09 mM

Table 1. Table presents the comparative binding energies and predicted IC_{50} values of the identified hits by Autodock software. N.D—not determined because the binding energy of MMV676603 was in positive range i.e., 0.18, hence, the software was not able to predict its IC_{50} value.

Molecular insights: unravelling interactions between identified leads and the enzyme. Protein-inhibitor interaction studies were performed to gain better insight into the binding mode of the compunds MMV676603 and MMV688704. As depicted in Fig. 5a, MMV676603 obstructs the catalytic center of PfUCHL3 by funneling into the binding groove of PfUCHL3. This complex is stabilized by the formation of a hydrogen bond with ASN61 and hydrophobic interactions with HIS164, PHE208, ASP179, LYS182, TYR56, VAL58 and ASP60 of PfUCHL3 (Fig. 5c). Similarly, MMV688704 aligns in the binding groove of PfUCHL3 and overpasses the catalytic center (Fig. 5b) by forming a hydrogen bond with ARG181 and hydrophobic interactions with ASN59, HIS164, ASP60, TYR56, VAL58 and ASN61 (Fig. 5d). On the contrary, both MMV676603

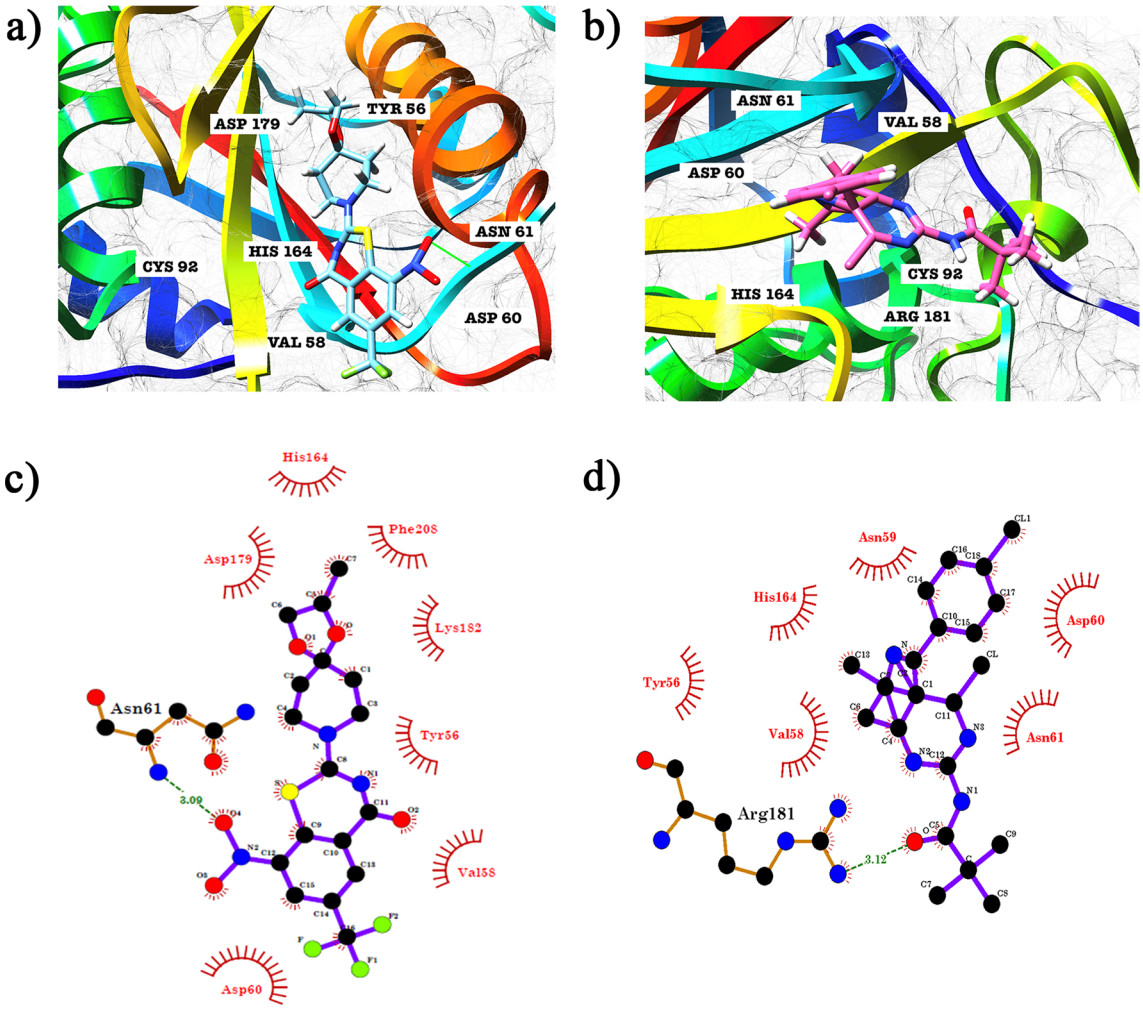

Figure 5. The two lead molecules docked to the active site cleft of PfUCHL3 (PDB ID: 2WE6): cartoon representation of predicted binding of (**a**) MMV676603 and (**b**) MMV688704 with PfUCHL3. 2-D ligand interaction maps of (**c**) MMV676603 and (**d**) MMV688704. Green lines depict hydrogen bonds and eye shaped residues exhibit hydrophobic interactions.

and MMV688704 sit in an entirely different groove (Fig. 6a,b) and show interactions with residues that do not play any interphase in enzymatic activity (Fig. 6c,d) and do not demonstrate any specific binding to human ortholog, supported by docking results. Hence, these results indicate the selective binding of the identified hits to PfUCHL3 over HsUCHL3 and provide scope for further refinement and lead optimization studies.

Anti-malarial effect of MMV676603 and MMV688704 on intra-erythrocytic stage of *P. falciparum*. Since PfUCHL3 is cardinal for the parasite, therefore, we hypothesized that the inhibitors of PfUCHL3 would be effective in inhibiting parasite growth. To test this, we determined the inhibitory effect of the identified hits against the asexual intra-erythrocytic stage of *P. falciparum 3D7* in culture using SYBR Green I assay. The standard anti-malarial, Chloroquine was used as an internal reference for validation of the assay. As expected, both the compounds were equally effective and caused complete inhibition of parasite growth at a concentration of 10 µM. Compounds MMV676603 and MMV688704 displayed a dose dependent inhibition of Chloroquine (CQ)-sensitive *P. falciparum 3D7* strain with IC_{50} values 450.5 ± 1.84 nM and 266.6 ± 1.77 nM, respectively (Fig. 7a,b).

In-vitro phenotypic and speed of action analysis of the two hit molecules. To investigate the effect of MMV676603 and MMV688704 on parasite growth and phenotype, ring stage parasites were treated with the compounds at ten-fold concentration of the IC_{50} value and observed at various intervals for 56 h. Cultures treated with MMV676603 and MMV688704 displayed the appearance of young trophozoites at 16 h, exhibiting a similarity with the control set. However, both MMV676603 and MMV688704 treated parasites were arrested at the late trophozoite stage with shrunken, less granular and condensed appearance of the parasite. In comparison to control, both MMV676603 and MMV688704 treatment caused substantial delay in the transition from trophozoite to schizont stage. This results in complete arrest of the parasite growth at later stages of the

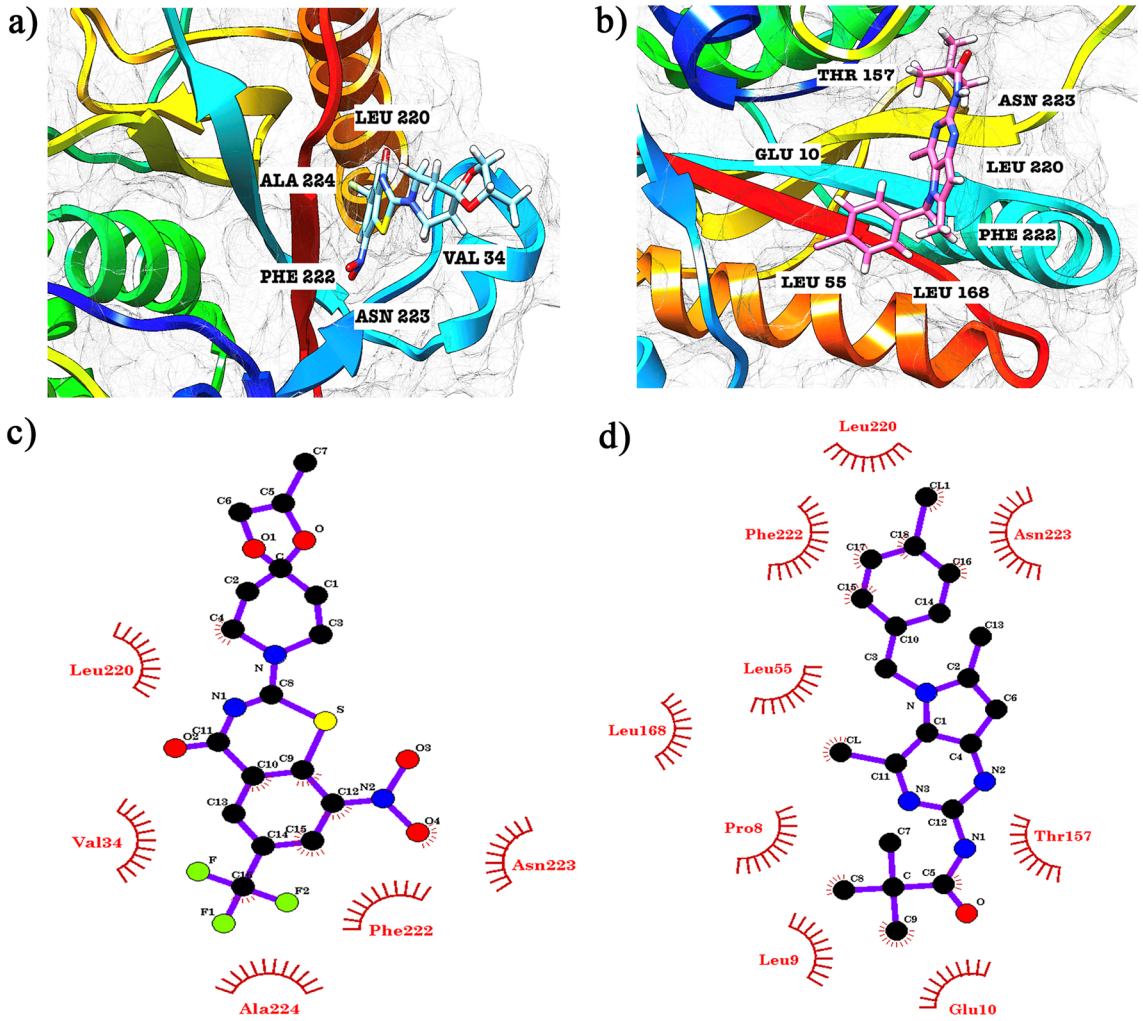

Figure 6. Leads docked to HsUCHL3 (PDB ID: 1XD3): cartoon representation of predicted binding of (**a**) MMV676603 and (**b**) MMV688704 with HsUCHL3. 2-D ligand interaction maps of (**c**) MMV676603 and (**d**) MMV688704. Green lines depict hydrogen bonds and eye shaped residues exhibit hydrophobic interactions.

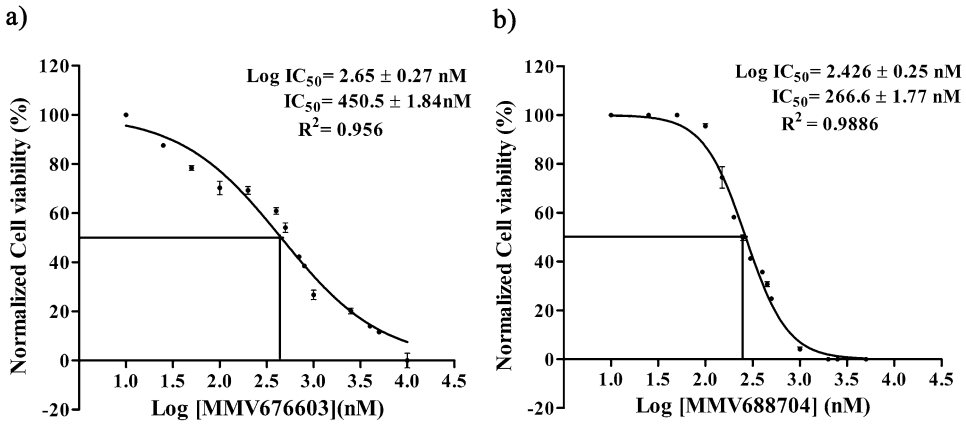

Figure 7. IC_{50} determination of MMV676603 and MMV688704 from Pathogen Box against blood stage of *P. falciparum* 3D7: dose–response curve indicating the Log IC_{50}, IC_{50} and R^2 values of (**a**) MMV676603 and (**b**) MMV688704 against asexual stages of *P. falciparum* 3D7. Inhibition at each data point is depicted as Mean ± S.D. of three independent experiments.

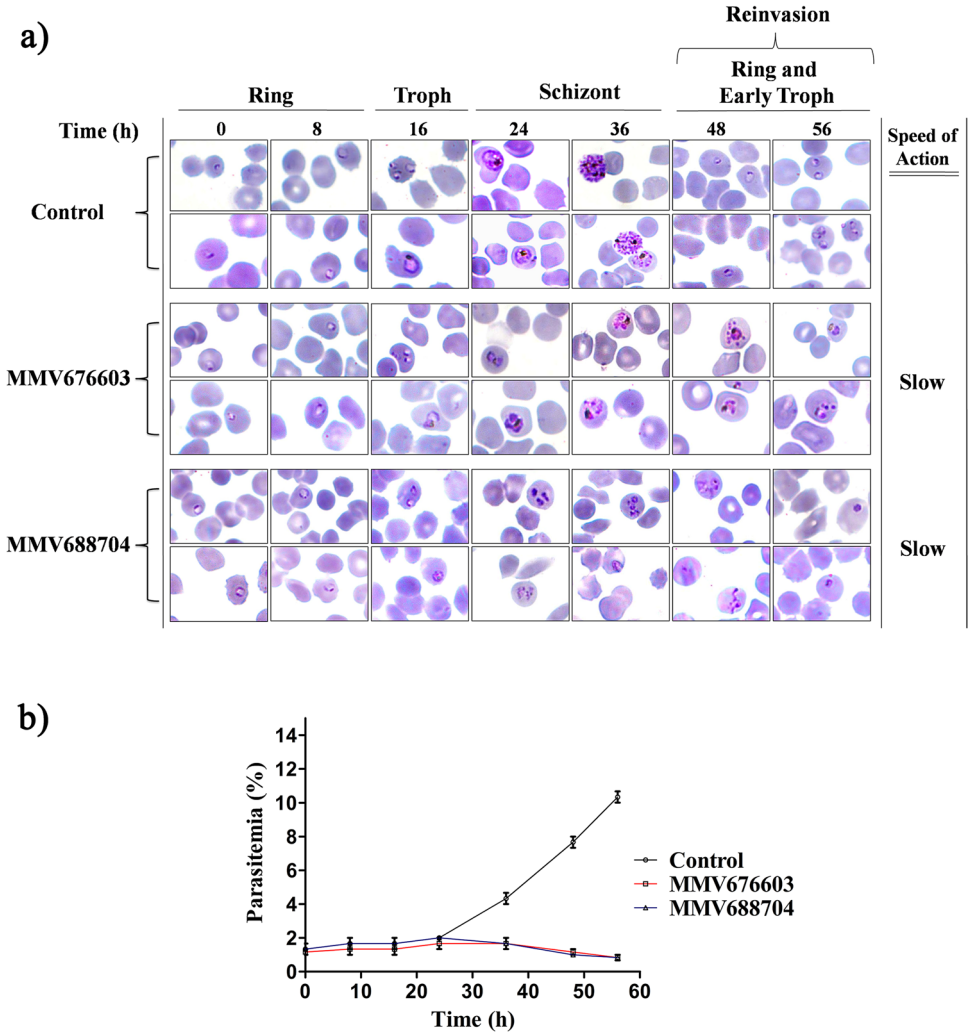

Figure 8. Effect of MMV676603 and MMV688704 on the growth and morphology of intraerythrocytic stage of *P. falciparum*, and assessment of their speed of action: synchronized *P. falciparum* 3D7 culture was treated with leads (MMV676603 and MMV688704) and their effect on parasite phenotype and growth was analyzed by (**a**) Giemsa stained blood smear micrographs at 0, 8, 16, 24, 36, 48 and 56 h (two representative images of each set). The speed of action of both the compounds (MMV676603 and MMV688704) was evaluated for one complete maturation cycle [starting from ring (0 h), trophozoite (16–24 h) to schizont (36 h)]. Both the compounds were considered as slow inhibitors as they hinder the parasite development at late stages (trophozoite and schizont). (**b**) The in-vitro reduction in parasitemia level was quantified and illustrated as a graph, indicating the parasitemia level as a function of parasite life cycle progression (time). Data are represented as Mean ± S.D.

parasite life cycle. Moreover, both MMV676603 and MMV688704 impeded erythrocyte reinvasion as indicated by absence of the new ring-stage parasite even at 56 h post drug incubation as shown in Fig. 8a. These results were further supported by quantification of parasitemia level at different time points, which revealed a continuous reduction in parasite count after 24 h accounting for almost ten-fold drop in parasitemia at 56 h (Fig. 8b). These results suggest that both MMV676603 and MMV688704 are slow acting inhibitors of parasite growth in culture (Fig. 8a).

Effect of MMV676603 and MMV688704 on ubiquitination levels. Considering the in-vitro inhibitory action of the two molecules against PfUCHL3 activity, we determined their effect on parasite ubiquitination level to ascertain that the parasiticidal activity of the identified compounds is mediated through PfUCHL3 inhibition. With this aim, asynchronous parasite culture was exposed to three times the IC_{50} concentration of the two inhibitors and ubiquitination levels were detected post treatment. Treatment with both MMV676603 and MMV688704 induced a significant accumulation of high-molecular weight ubiquitin conjugates. In comparison to the vehicle control set, treatment with MMV676603 displayed the highest levels of ubiquitination laddering, followed by MMV688704 (Fig. 9). In contrast, Chloroquine, a known antimalarial exhibited negligible effect on the parasite ubiquitination levels (Fig. 9), indicating that these compounds alter PfUCHL3 activity for effective parasite killing.

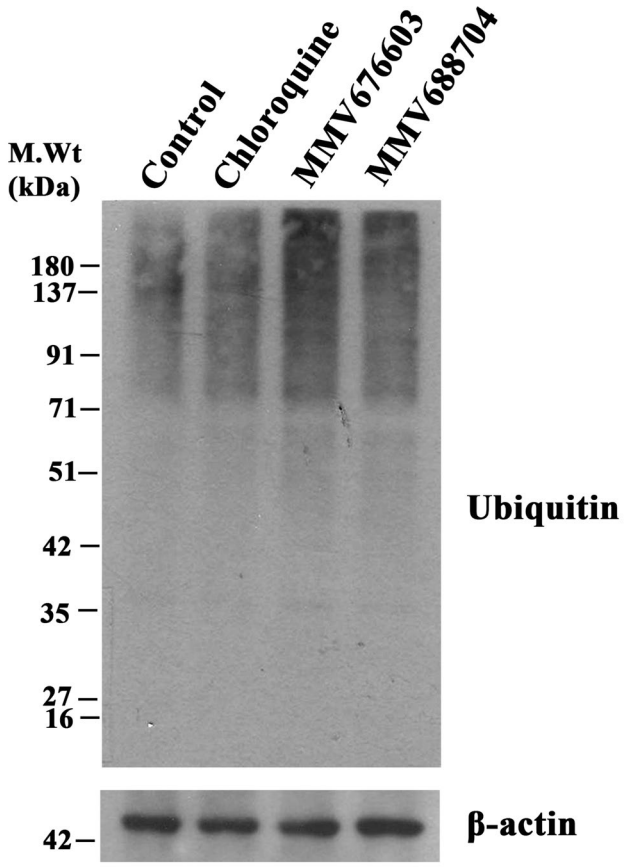

Figure 9. Effect of leads on ubiquitination levels: asynchronous *P. falciparum* culture was treated with vehicle control (Lane 1), Chloroquine (Lane 2) and identified compounds (MMV676603 (Lane 3), MMV688704 (Lane 4)). Following treatment, parasites were lysed and equal amount of parasite lysate was subjected to SDSPAGE and immunoblotting was carried out with ubiquitin antibody for ubiquitination levels. β-actin was kept as loading control. The experiment was performed atleast thrice with a respresentative image shown as figure. Full blots are provided in Supplementary Fig. S2.

Compound no.	Compound ID	*P. falciparum* 3D7 IC_{50} (nM)	HEK-293T IC_{50} (μM)	HepG2 IC_{50} (μM)	Selective Index (HEK-293T)	Selective Index (HepG2)
1	**MMV676603**	450.5 ± 1.84	> 20	> 20	50	50
2	**MMV688704**	266.6 ± 1.77	> 20	> 20	100	100

Table 2. In-vitro activity of the two hits identified from Pathogen Box against parasite and mammalian cell culture.

Cytotoxicity against mammalian cell lines. To demonstrate that the anti-parasitic effect of MMV676603 and MMV688704 was not due to general toxicity, the compound mediated cytotoxic effect was determined in the human hepatic cell line (HepG2) and human embryonic kidney cells (HEK-293T) with the help of MTT assay. No cytotoxicity was observed up to a concentration of 20 μM (100 times the effective concentration) (Fig. S3). Furthermore, as summarized in Table 2, compound MMV676603 and MMV688704 displayed a Selectivity Index of 50 and 100, respectively, presumably indicating a high anti-parasitic selective profile of these hits.

Discussion

Regardless of the extensive efforts to combat this infectious disease, malaria continues to torment the world with its severity and complexity[69]. Limited protection by licensed vaccine and development of accelerated resistance to current clinical anti-malarials has overcome the efforts to contain this disease[70,71]. Such a scenario, stimulates an urgent need for new drug discovery programs to mitigate associated problems and develop new and cost effective anti-malarial therapies with least side effects.

DUBs are a group of highly sophisticated enzymes known to regulate a number of cellular functions and their deregulation contribute to the development of severe clinical manifestations[28,72]. Likewise, compelling evidences from literature highlight the critical importance of DUBs in parasite biology. However, till recent times, studies

exploiting DUBs as a therapeutic target in *Plasmodium* are limited. PfUCHL3 is one such promising member of *Plasmodium* deubiquitinase family, whose absence exhibits a lethal effect on parasite survival, thereby, validating its utmost importance as a therapeutic target[46]. A report by Franco et al., identified inhibitors against PfUCHL3 from the ZINC database by virtual screening[73]. Unfortunately, the study lacked enzymatic validation and biological assay of the identified hits. Even though, PfUCHL3 shares some identity with HsUCHL3, the subtle differences in the active site pocket and substrate binding groove could serve as a fundamental scaffold for the development of selective therapeutics[55]. Therefore, in the present study, we focused to query Pathogen Box compounds for identification of novel PfUCHL3 inhibitors as potent anti-malarials.

Herein, we performed targeted docking in search of selective inhibitors of PfUCHL3 over HsUCHL3 using AutoDock suite. The molecules, exhibiting selectivity towards *P. falciparum* UCHL3 and displaying drug like properties were evaluated for their in vitro enzyme inhibition assay at 100 µM. Interestingly, MMV676603 and MMV688704 were identified as potent inhibitors that potentially impeded PfUCHL3 activity at sub-micromolar concentration, which was in close association with the predicted in-silico IC_{50} values and was further supported by predicted dock score values. We also performed a detailed analysis of the docked complexes to gain better insight into the binding mechanism of both the hits. Notably, MMV676603 blocks the binding pocket of PfUCHL3 by residing in the binding groove with its azapiro ring facing the catalytic unit (CYS92, HIS164 and ASP179) whereas the benzo ring faces the crossover loop. Such affirmative orientation positions the hydrogen acceptor and donors in the close vicinity thus contributing to the formation of strong non-covalent interactions, including hydrogen bonds with the catalytic triad along with ASP60, ASN61, van der waal interactions with PHE208 and TYR56 and ionic interactions with LYS182. The presence of three fluorines in MMV676603 further strengthens these interactions, thereby, enhancing the selectivity and permeability. Incidentally, fluorination of ligand molecules is a common practice to elevate the potency of the inhibitors. Whilst, these are short interactions, yet they impart a significant effect on protein ligand binding[74]. On the contrary, MMV676603 lacks proper orientation in the binding groove and interacts with the amino acid residues (LEU220-ALA224) lining the C-terminal region of HsUCHL3. Together, these collated evidences advocate for more proficient suppressive effects of MMV676603 on PfUCHL3 activity as compared to its mammalian ortholog. Additionally, MMV688704 also aligns itself in the binding groove of PfUCHL3 with the tail of the benzene ring facing the crossover loop and the pyrimidine ring aligns towards the catalytic center of PfUCHL3. This allows MMV688704 to form a strong network of non-covalent interactions with the amino acid residues surrounding the binding pocket. In contrast, the horizontal orientation of the MMV688704 (facing the C-terminal region) in HsUCHL3 hampers its interaction with the catalytic groove, thereby, impeding its potency towards human UCHL3. Both the compounds obey all druglikeliness parameters as depicted by bioavailability radar and even exhibit zero violation of Lipinski rule of five, which makes them suitable for oral absorption.

The compounds MMV676603 and MMV688704 were evaluated for their anti-malarial potential and compounds MMV676603 and MMV688704 were highly efficient against *P. falciparum* 3D7 (CQ-sensitive strain) in culture with an IC_{50} value of 450.5 ± 1.84 nM and 266.6 ± 1.77 nM, respectively. Both MMV676603 and MMV688704 displayed asexual stage dependent growth inhibition after prolonged exposure of drug (after 24 h) and caused phenotypic and developmental aberrations in parasites. The treated parasite was completely arrested at late stages (trophozoites/schizont) with a compact and shrunken appearance as evidenced by lack of ring stage even after 56 h. The trophozoite stage marks the initiation of a highly replicative phase in the parasite life cycle, which indicates high dependency on the ubiquitin regulatory machinery for invasion and differentiation[16]. Therefore, it can be envisaged that DUBs like PfUCHL3 might regulate the critical processes in late asexual stages of the parasite and its inhibition by MMV676603 and MMV688704 hampers the parasite growth by altering the protein homeostasis and other essential pathways. Additionally, to affirm whether the biological action of these compounds is exerted through PfUCHL3 inhibition, the parasite ubiquitination levels were determined upon exposure to the selected hits. As compared to control and CQ, a known antimalarial with different mode of action, both MMV676603 and MMV688704 treated parasites exhibited a marked increase in the ubiquitination levels, thereby, suggesting their inhibitory role towards the deubiquination process. In comparison to MMV676603, a less intense ubiquitination pattern in MMV688703 treated set could be an attribute of differential impact on PfUCHL3 activity, rendering its dexterity to curb the deubiquitination event in the parasite milieu. Despite such variable biological effects, the enhanced ubiquitination laddering in compounds treated sets provide compelling evidences for PfUCHL3-mediated parasite killing by the identified hits. This, coupled with other results, make it very likely that the compounds MMV676603 and MMV688704 might be equally effective against the resistant strains of the parasite and possibly be used as an adjunct therapeutics in ACTs., Pathogen Box classifies MMV676603 and MMV688704 against tuberculosis and toxoplasmosis, respectively. However, this is the first report of their identification as an anti-malarial. MMV676603 belongs to the nitrobenzothiazinones family and is effective against the clinical isolates of tuberculosis[75]. Currently, it is under pre-clinical trials for the treatment of drug-resistant tuberculosis[76]. Some studies have also identified its potential against *N. brasiliensi*[77] *a*nd Corynebacterineae[78]. Alongside, this drug acts by forming a covalent bond with CYS387 of DprE1of an oxidoreductase enzyme that is vital for cell wall arabinan synthesis and ultimately death[78,79]. Consequently, we can infer that MMV676603 inhibits PfUCHL3 activity by altering the key interaction of cysteine residue present in the active site pocket of the enzyme. Such inhibition renders the enzyme non-functional by obstructing the overall parasite growth. In contrast, MMV688704 belongs to the family of pyrimidine, mainly known as DHFR inhibitors[80] with minimal evidence of it as anti-toxoplasmosis. In our study, MMV688704 displayed a better efficacy against the parasites in culture with enzyme inhibition at the micro molar range, which could be a result of an additional mode of action. Hence, the results necessitate further lead optimization and chemical engineering to improve its efficacy. These studies were further complemented by cytotoxicity assay on mammalian cell lines. Expectedly, compound MMV676603 and MMV688704 selectively inhibited parasites over the mammalian cell lines (HEK-293T and HepG2 cells) with S.I value of more than 50, which was in corroboration with our in-silico

studies. However, in-vivo and dynamic mechanistic studies are warranted to provide a better insight into the potential of PfUCHL3 as a therapeutic target. Concurrently, our study identified MMV676603 and MMV688704 as promising antimalarial with appreciable inhibition of PfUCHL3 activity.

Conclusion

The present study represents first comprehensive attempt to repurpose the collection of MMV Pathogen Box compounds targeting UCHL3 of *P. falciparum* for the development of anti-malarial chemotherapy. In this study, we identified two novel promising non-cytotoxic small molecules, MMV676603 and MMV688704, as PfUCHL3 antagonists with biological activity against *P. falciparum* as an outcome of a stringent screening. In comparison to MMV676603, MMV688704 was found to be more potent against the parasite, but less effective against recombinant PfUCHL3. Therefore, it is tempting to dissect its probable mode of action. Besides this, both MMV676603 and MMV688704 hold the potential as potent anti-malarial. Therefore, improvement towards selectivity for PfUCHL3 over human ortholog and in-vivo studies will complement these findings. The outcome of this study provides a scaffold for future optimization of more specific, effective and selective compounds with its implication as a therapeutic as well as a tool to identify the biological functions of the enzyme. Overall, inhibitors targeting the UCHL3 family of DUBs can enlighten the drug development path and discovery against a range of parasitic and infectious diseases.

Material and methods

Pathogen Box compounds. The Pathogen Box was procured from Medicine for Malaria Venture (MMV) foundation (Geneva, Switzerland). The library of compounds was supplied in 96-well microtitre plate at a concentration of 10 mM in dimethyl sulfoxide (DMSO) (10 µL) and further dilutions were prepared according to MMV instructions. The details about plate layout, chemical formula and other biological activity are available online as Pathogen Box supporting information in a form of an Excel spreadsheet (https://www.pathogenbox.org/about-pathogen-box/supporting-information).

Constructs, antibodies and chemicals. Bacterial expression vector encoding PfUCHL3 was a generous gift from Dr. Hidde Ploegh, Boston Children's Hospital, MA and Katerina Artavanis-Tsakonas, Department of Pathology, University of Cambridge, Cambridge, UK. The gene encoding HsUCHL3 was amplified from HEK-293T cDNA using 5′-GGT CAT ATG GAG GGT CAA CGC TGG CTG-3′ and 5′-CCC AAG CTT CTA TGC TGC AGA AAG AGC-3′ as forward and reverse primer, respectively. The amplified gene was cloned between NdeI and HindIII of pET28a(+) as a N-terminus 6 X His tag. The gene sequences were verified by DNA sequencing. Anti-ubiquitin and anti-β-actin antibodies were purchased from Santa Cruz Biotechnology Inc. (Santa Cruz, CA, USA). Isopropyl β-D-1-thiogalactopyranoside (IPTG) was obtained from Bio Basic Inc. (Markham, Canada). SYBR Green I, penicillin and nickel nitrilotriacetic acid (Ni–NTA) beads were procured from Thermo Scientific (Rockford IL, USA). Dithiothreitol (DTT) and hypoxanthine were obtained from Sigma (St. Louis, MO, USA). Powdered RPMI-1640 and Albumax II were obtained from GIBCO (ThermoFisher Scientific, Waltham, MA, USA). DMEM and streptomycin were purchased from Invitrogen (Carlsbad, CA, USA). All other reagents were of analytical grade.

Heterologous expression and purification of recombinant proteins. Expression vector encoding PfUCHL3 and HsUCHL3 was transformed in *E. coli BL21(DE3)* cells. Protein expression and purification of the recombinant proteins were performed as described previously with slight modification[46]. In brief, protein expression was induced with 1 mM IPTG for 16 h at 30 °C. The cells were harvested and the pellet was lysed with lysis buffer (50 mM Tris, 150 mM NaCl, 2 mM DTT) containing protease inhibitor cocktail, lysozyme and DNase. The lysate was sonicated and the clear lysate was loaded onto a pre-equilibrated Ni–NTA column and protein was eluted with increasing concentration of imidazole hydrochloride. Subsequently, the eluants were subjected to size exclusion chromatography (AKTA Prime, GE Healthcare, Björkgatan, Uppsala, Sweden) and the fractions were collected and purity of the protein was determined by SDS-PAGE analysis.

Structure based virtual screening (SBVS). The dataset comprising of 400 molecules from MMV, Geneva were docked against the active site of PfUCHL3 and its human ortholog whose crystal structure was retrieved from Protein Data Bank (PDB ID: 2WE6 and 1XD3 respectively). Autodock Racoon software[81] was used for docking. Before commencing for docking, the protein and ligands were prepared separately. Water molecules and cofactors were removed from the protein. However, the SMILES of 400 compounds were used to retrieve the 2D structures from ChEMBL database, followed by their conversion to PDB via Pymol and lastly to the PDBQT format. Subsequently, the grid was generated by keeping the active site residues (CYS92, HIS164 and ASP179) of PfUCHL3 as highlights, which are dissimilar in positioning when compared with human UCHL3 whose binding pocket comprises of CYS95, HIS169 and ASP184. Top 100 compounds having a comparative binding energy value of ≥ 3 kcal/mol were selected for ADME analysis.

ADME screening. The assortment of flawed molecular entities in the early phases of drug discovery diminishes the error rate and increases the efficacy in the initial stage. Hence, the pharmacokinetic activities of the leads were estimated using SWISS ADME[82]. Only drug-like candidates with zero violation of Lipinski rule of five and with easy absorption, distribution, metabolism and excretion were taken forward.

In-vitro DUB assay. The selected compounds were initially screened against recombinant PfUCHL3 at a concentration of 100 µM using fluorimetric assay as described by Artavanis et al.[46] with relevant modification. In brief, the assay was performed in a 60 µl reaction volume containing 10 pM of enzyme in reaction buffer (50 mM Tris–Cl, pH-8.0, 150 mM NaCl, 2 mM DTT, 2 mM EDTA and 0.1 mg/mL BSA) and 100 µM of compounds. The fluorogenic peptide substrate Ub-AMC (Ubiquitin C-terminal tagged 7-amido-4-methylcoumarin)(Boston Biochem,Cambridge, MA, USA) was added at a final concentration of 125 nM and the release of AMC was continuously monitored (Excitation: 485 nm and Emission: 535 nm) for a period of 30 min at 25 °C. The enzyme inhibition assay for each compound was performed in triplicates. The compounds inhibiting ≥ 50% of PfUCHL3 activity were identified as potent hits. The IC_{50} of best compounds was determined through the dose–response workspace of GraphPad Prism Software (GraphPad Co. Ltd., San Diego, CA, USA).

In-vitro culturing and synchronization of parasite. *Plasmodium falciparum 3D7* was cultured with human O^+ human erythrocyte (5% hematocrit) in RPMI-1640 (Gibco, ThermoFisher Scientific, Waltham, MA, USA) medium supplemented with 0.5% (w/v) Albumax (Gibco, ThermoFisher Scientific, Waltham, MA, USA), Hypoxanthine (50 mg/L), Gentamicin (10 mg/L) and Ampicillin (10 mg/L) in mixed gas environment (5% O_2, 5% CO_2 and 90% N_2) at 37 °C[83]. Human whole blood was procured from the Rotary Blood Bank, New Delhi. Under sterile conditions, erythrocytes were obtained by removal of plasma and peripheral blood mononuclear cells (PBMCs) using histopaque gradient. Parasitemia levels were routinely assessed using Giemsa staining of blood smears. Synchronization was performed using the sorbitol lysis method[84]. The parasite culture was treated with 5% D-sorbitol for 10 min at 37 °C for the enrichment of ring stage parasite. The culture was pelleted by centrifugation and washed thrice with media. In addition, the high synchrony level of the parasite was maintained by performing two consecutive sorbitol treatments at an interval of 4 h. The parasite was visualized by microscopic analysis of Giemsa stained blood smears.

Drug susceptibility assay for asexual stages of *P. falciparum*. In-vitro anti-malarial efficacy of compounds was determined by SYBR-Green I based proliferation assay as reported previously[85] with slight modification. In brief, various dilutions of test compounds (10 µL) were added to 96-well microdilution plates and asynchronous parasite culture at 4% hematocrit and 0.5% parasitemia was added to pre-dosed plates in a total volume of 100 µL. After 48 h of incubation at 37 °C under 90% N_2, 5% CO_2 and 5% O_2, the plates were frozen at − 20 °C for an additional 24 h. Subsequently, plates were thawed and 100 µL of lysis buffer (20 mM Tris base, 5 mM EDTA, 0.0008% (v/v) Triton X-100, 0.008% (m/v) saponin, pH 8.0) containing 0.002% (v/v) SYBR Green I was added. Plates were incubated at 37 °C for 1 h and fluorescence readings were taken using Infinite M 200 PRO microplate reader (TECAN, Männedorf, Switzerland) with excitation and emission wavelengths of 485 nm and 535 nm, respectively. The half maximal inhibitory concentration (IC_{50}) was determined via GraphPad PRISM 5.0 using non-linear regression analysis.

Phenotypic evaluation and speed of action studies. Synchronized culture containing ring stage parasites at 1% parasitemia and 2% hematocrit was treated with test compounds at tenfold the IC_{50} concentration. After addition of compounds, the parasitemia level was quantified and morphological changes were studied by microscopic analysis of Giemsa stained thin blood smear at 0, 8, 16, 24, 36, 48 and 56 h. The speed of action of the compounds was determined on the basis of their effect on the early or late stage of the erythrocytic stages of the parasite as described by Terquille et al.[86].

Effect of selected hits on parasite ubiquitination levels. Asynchronus parasite cultures at 5% hematocrit and 4–5% parasitemia were incubated in the absence (vehicle control) or presence of three times the IC_{50} concentration of the identified compounds or Chloroquine (CQ) for 24 h at 37 °C. Post treatment, cultures were harvested and pellets were extracted with 0.1% (w/v) saponin for 15 min on ice. Cells were pelleted and parasite pellets were washed with PBS until the supernatant became clear. Parasite pellets were resuspended in RIPA buffer (150 mM NaCl, 1% Nonidet P-40, 0.5% sodium deoxycholate, 0.1% SDS, 50 mM Tris pH 8.0) and lysed on ice for 45 min, followed by mild 6 cycles of sonication (2 s On and 2 s Off) and the clear lysate was obtained post centrifugation at 13,800×*g* for 15 min at 4 °C. Protein concentration was estimated by Bradford and an equal amount of parasite lysates were resolved on SDS-PAGE and subjected to immunodetection using anti-ubiquitin antibody and anti β-actin antibody (loading control).

Cytotoxicity assessment against mammalian cell lines. HepG2 (human hepatocellular carcinoma) and HEK-293T (human embryonic kidney) cells were cultured DMEM (Invitrogen, Carlsbad, CA) medium supplemented with 10% fetal bovine serum and antibiotics (100 U/mL of penicillin and 100 mg/mL streptomycin) in a humidified 5% CO_2 chamber at 37 °C.The cytotoxicity of top hits was assessed against HepG2 and HEK-293T cells using MTT assay as described previously[87]. In brief, cells were seeded in a 96 well microplate and incubated for 24 h at 37 °C in a CO_2 incubator. After 24 h, cells were exposed to different dilutions of drugs (prepared in respective medium) for 24 h. Post incubation, MTT was added and the plate was incubated at 37 °C for 4 h. Subsequently, the supernatant was removed and DMSO was added to solubilize the formazan crystals. Absorbance was measured at 570 nm using an Infinite M 200 PRO microplate reader (Tecan, Switzerland) with the Magellan 7 software. IC_{50} values were determined by nonlinear regression analysis GraphPad Prism 5 software (GraphPad Software, San Diego, CA).

Selective Index (S. I.). Selective Index of the top hits was determined by application of the following formula[62]:

$$S.I_{P.falciparum} = IC_{50(\text{HEK}-293\text{T or HepG2})}/IC_{50(P.falciparum)}$$

Statistical analysis. Preparation of graphs and statistical analysis of data were performed using Prism 5 software (GraphPad Software, San Diego, CA). A non-linear regression sigmoidal dose dependent curve fit was applied to dose–response data for the determination of half maximal concentrations (IC_{50}s). All data are presented as Mean ± S.D. from atleast three independent experiments.

Ethical declaration. Parasite culture was maintained as per safety guidelines of the Department of Biotechnology, Ministry of Science and Technology, Government of India and has been approved by the Institutional Biosafety Committee of the University of Delhi, South Campus, New Delhi (Ref. no.-155/AN/Biochem/UDSC/IBSC/02/08/2019).

Received: 18 March 2021; Accepted: 22 December 2021
Published online: 18 January 2022

References

1. World Health Organization. World malaria report 2020. World Health Organization (WHO), 299 (2020).
2. Snow, R. W., Guerra, C. A., Noor, A. M., Myint, H. Y. & Hay, S. I. The global distribution of clinical episodes of *Plasmodium falciparum* malaria. *Nature* **434**, 214–217 (2005).
3. Bhatt, S. *et al.* The effect of malaria control on *Plasmodium falciparum* in Africa between 2000 and 2015. *Nature* **526**, 207–211 (2015).
4. Flannery, E. L., Chatterjee, A. K. & Winzeler, E. A. Antimalarial drug discovery—Approaches and progress towards new medicines. *Nat. Rev. Microbiol.* **11**, 849–862 (2013).
5. Galatas, B., Bassat, Q. & Mayor, A. Malaria parasites in the asymptomatic: Looking for the hay in the haystack. *Trends Parasitol.* **32**, 296–308 (2016).
6. Phyo, A. P. *et al.* Emergence of artemisinin-resistant malaria on the western border of Thailand: A longitudinal study. *Lancet* **379**, 1960–1966 (2012).
7. Imwong, M. *et al.* An outbreak of artemisinin resistant falciparum malaria in Eastern Thailand. *Sci. Rep.* **5**, 17412 (2015).
8. Ashley, E. A. *et al.* Spread of artemisinin resistance in *Plasmodium falciparum* malaria. *N. Engl. J. Med.* **371**, 411–423 (2014).
9. Fairhurst, R. M. Understanding artemisinin-resistant malaria: what a difference a year makes. *Curr. Opin. Infect. Dis.* **28**, 417–425 (2015).
10. Blasco, B., Leroy, D. & Fidock, D. A. Antimalarial drug resistance: Linking *Plasmodium falciparum* parasite biology to the clinic. *Nat. Med.* **23**, 917–928 (2017).
11. White, N. J. Does antimalarial mass drug administration increase or decrease the risk of resistance?. *Lancet Infect. Dis.* **17**, e15–e20 (2017).
12. RTS,S Clinical Trials Partnership. Efficacy and safety of RTS, S/AS01 malaria vaccine with or without a booster dose in infants and children in Africa: Final results of a phase 3, individually randomised, controlled trial. *Lancet* **386**, 31–45 (2015).
13. Bharti, H., Singal, A., Raza, M., Ghosh, P. & Nag, A. Ionophores as potent anti-malarials: A miracle in the making. *Curr. Top. Med. Chem.* **18**, 2029–2041 (2018).
14. Ganesan, K. *et al.* A genetically hard-wired metabolic transcriptome in Plasmodium falciparum fails to mount protective responses to lethal antifolates. *PLoS Pathog.* **4**, e1000214 (2008).
15. Chung, D.-W.D., Ponts, N., Cervantes, S. & Le Roch, K. G. Post-translational modifications in Plasmodium: More than you think!. *Mol. Biochem. Parasitol.* **168**, 123–134 (2009).
16. Ponts, N. *et al.* Unraveling the ubiquitome of the human malaria parasite. *J. Biol. Chem.* **286**, 40320–40330 (2011).
17. Nair, S. C. *et al.* A *Plasmodium yoelii* HECT-like E3 ubiquitin ligase regulates parasite growth and virulence. *Nat. Commun.* **8**, 1–14 (2017).
18. Green, J. L. *et al.* Ubiquitin activation is essential for schizont maturation in *Plasmodium falciparum* blood-stage development. *PLoS Pathog.* **16**, e1008640 (2020).
19. Aminake, M. N., Arndt, H.-D. & Pradel, G. The proteasome of malaria parasites: A multi-stage drug target for chemotherapeutic intervention?. *Int. J. Parasitol. Drugs Drug Resist.* **2**, 1–10 (2012).
20. Jain, J., Jain, S. K., Walker, L. A. & Tekwani, B. L. Inhibitors of ubiquitin E3 ligase as potential new antimalarial drug leads. *BMC Pharmacol. Toxicol.* **18**, 1–10 (2017).
21. Ng, C. L., Fidock, D. A. & Bogyo, M. Protein degradation systems as antimalarial therapeutic targets. *Trends Parasitol.* **33**, 731–743 (2017).
22. Komander, D. & Rape, M. The ubiquitin code. *Annu. Rev. Biochem.* **81**, 203–229 (2012).
23. Eytan, E., Ganoth, D., Armon, T. & Hershko, A. ATP-dependent incorporation of 20S protease into the 26S complex that degrades proteins conjugated to ubiquitin. *Proc. Natl. Acad. Sci. USA* **86**, 7751–7755 (1989).
24. Kallio, P. J., Wilson, W. J., O'Brien, S., Makino, Y. & Poellinger, L. Regulation of the hypoxia-inducible transcription factor 1alpha by the ubiquitin-proteasome pathway. *J. Biol. Chem.* **274**, 6519–6525 (1999).
25. Koepp, D. M., Harper, J. W. & Elledge, S. J. How the cyclin became a cyclin: Regulated proteolysis in the cell cycle. *Cell* **97**, 431–434 (1999).
26. Guo, W. *et al.* Differential regulation of components of the ubiquitin-proteasome pathway during lens cell differentiation. *Invest. Ophthalmol. Vis. Sci.* **45**, 1194–1201 (2004).
27. Dupre, D. J. *et al.* Trafficking, ubiquitination, and down-regulation of the human platelet-activating factor receptor. *J. Biol. Chem.* **278**, 48228–48235 (2003).
28. Shanmugham, A. & Ovaa, H. DUBs and disease: Activity assays for inhibitor development. *Curr. Opin. Drug Discov. Devel.* **11**, 688–696 (2008).
29. Wang, J. & Maldonado, M. A. The ubiquitin-proteasome system and its role in inflammatory and autoimmune diseases. *Cell Mol. Immunol.* **3**, 255–261 (2006).

30. Richardson, P., *et al.* The treatment of relapsed and refractory multiple myeloma. *Hematol. Am. Soc. Hematol. Educ. Program.* **1**, 317–323 (2007).
31. Srikanth, M., Davies, F. E. & Morgan, G. J. An update on drug combinations for treatment of myeloma. *Expert Opin. Investig. Drugs* **17**, 1–12 (2008).
32. Gupta, I., Aggarwal, S., Singh, K., Yadav, A. & Khan, S. Ubiquitin Proteasome pathway proteins as potential drug targets in parasite *Trypanosoma cruzi*. *Sci. Rep.* **8**, 1–12 (2018).
33. Qiu, J. & Luo, Z.-Q. Hijacking of the host ubiquitin network by *Legionella pneumophila*. *Front. Cell. Infect. Microbiol.* **7**, 487 (2017).
34. Harrigan, J. A., Jacq, X., Martin, N. M. & Jackson, S. P. Deubiquitylating enzymes and drug discovery: Emerging opportunities. *Nat. Rev. Drug Discov.* **17**, 57 (2018).
35. Datta, G., Hossain, M. E., Asad, M., Rathore, S. & Mohmmed, A. *Plasmodium falciparum* OTU-like cysteine protease (PfOTU) is essential for apicoplast homeostasis and associates with noncanonical role of Atg8. *Cell. Microbiol.* **19**, e12748 (2017).
36. Prudhomme, J. *et al.* Marine actinomycetes: A new source of compounds against the human malaria parasite. *PLoS ONE* **3**, e2335 (2008).
37. Reynolds, J. M., El Bissati, K., Brandenburg, J., Gunzl, A. & Mamoun, C. B. Antimalarial activity of the anticancer and proteasome inhibitor bortezomib and its analog ZL3B. *BMC Clin. Pharmacol.* **7**, 13 (2007).
38. Czesny, B., Goshu, S., Cook, J. L. & Williamson, K. C. The proteasome inhibitor epoxomicin has potent *Plasmodium falciparum* gametocytocidal activity. *Antimicrob. Agents Chemother.* **53**, 4080–4085 (2009).
39. Lindenthal, C., Weich, N., Chia, Y. S., Heussler, V. & Klinkert, M. Q. The proteasome inhibitor MLN-273 blocks exoerythrocytic and erythrocytic development of Plasmodium parasites. *Parasitology* **131**, 37–44 (2005).
40. Edelmann, M. J. & Kessler, B. M. Ubiquitin and ubiquitin-like specific proteases targeted by infectious pathogens: Emerging patterns and molecular principles. *Biochim. Biophys. Acta* **1782**, 809–816 (2008).
41. Hunt, P. *et al.* Gene encoding a deubiquitinating enzyme is mutated in artesunate- and chloroquine-resistant rodent malaria parasites. *Mol Microbiol* **65**, 27–40 (2007).
42. Hunt, P. *et al.* Experimental evolution, genetic analysis and genome re-sequencing reveal the mutation conferring artemisinin resistance in an isogenic lineage of malaria parasites. *BMC Genom.* **11**, 499 (2010).
43. Hamilton, M. J., Lee, M. & Le Roch, K. G. The ubiquitin system: An essential component to unlocking the secrets of malaria parasite biology. *Mol. Biosyst.* **10**, 715–723 (2014).
44. Ponts, N. *et al.* Deciphering the ubiquitin-mediated pathway in apicomplexan parasites: A potential strategy to interfere with parasite virulence. *PLoS ONE* **3**, e2386 (2008).
45. Wang, L. *et al.* Characterization of the 26S proteasome network in *Plasmodium falciparum*. *Sci. Rep.* **5**, 17818 (2015).
46. Artavanis-Tsakonas, K. *et al.* Characterization and structural studies of the *Plasmodium falciparum* ubiquitin and Nedd8 hydrolase UCHL3. *J. Biol. Chem.* **285**, 6857–6866 (2010).
47. Mtango, N. R., Sutovsky, M., Vandevoort, C. A., Latham, K. E. & Sutovsky, P. Essential role of ubiquitin C-terminal hydrolases UCHL1 and UCHL3 in mammalian oocyte maturation. *J. Cell Physiol.* **227**, 2022–2029 (2012).
48. Liao, C. *et al.* UCHL3 regulates topoisomerase-induced chromosomal break repair by controlling TDP1 proteostasis. *Cell Rep.* **23**, 3352–3365 (2018).
49. Nishi, R. *et al.* The deubiquitylating enzyme UCHL3 regulates Ku80 retention at sites of DNA damage. *Sci. Rep.* **8**, 17891 (2018).
50. Setsuie, R., Suzuki, M., Tsuchiya, Y. & Wada, K. Skeletal muscles of Uchl3 knockout mice show polyubiquitinated protein accumulation and stress responses. *Neurochem. Int.* **56**, 911–918 (2010).
51. Zhang, M. H. *et al.* UCHL3 promotes ovarian cancer progression by stabilizing TRAF2 to activate the NF-kappaB pathway. *Oncogene* **39**, 322–333 (2020).
52. Li, T. T. & Wang, H. J. UCH-L3 expression in epithelial ovarian cancer and its clinical significance. *Sichuan Da Xue Xue Bao Yi Xue Ban* **50**, 556–560 (2019).
53. Song, Z. *et al.* UCHL3 promotes pancreatic cancer progression and chemo-resistance through FOXM1 stabilization. *Am. J. Cancer Res.* **9**, 1970–1981 (2019).
54. Filatova, E. V. *et al.* Expression analysis of genes of ubiquitin-proteasome protein degradation system in MPTP-induced mice models of early stages of Parkinson's disease. *Dokl. Biochem. Biophys.* **456**, 116–118 (2014).
55. Popp, M. W., Artavanis-Tsakonas, K. & Ploegh, H. L. Substrate filtering by the active site crossover loop in UCHL3 revealed by sortagging and gain-of-function mutations. *J. Biol. Chem.* **284**, 3593–3602 (2009).
56. Li, H. *et al.* Structure- and function-based design of Plasmodium-selective proteasome inhibitors. *Nature* **530**, 233–236 (2016).
57. Booker, M. L. *et al.* Novel inhibitors of *Plasmodium falciparum* dihydroorotate dehydrogenase with anti-malarial activity in the mouse model. *J. Biol. Chem.* **285**, 33054–33064 (2010).
58. Davis, M. I. *et al.* Identification of novel *Plasmodium falciparum* hexokinase inhibitors with antiparasitic activity. *Antimicrob. Agents Chemother.* **60**, 6023–6033 (2016).
59. Austin, B. A. & Gadhia, A. D. New therapeutic uses for existing drugs. *Adv. Exp. Med. Biol.* **1031**, 233–247 (2017).
60. Breckenridge, A. & Jacob, R. Overcoming the legal and regulatory barriers to drug repurposing. *Nat. Rev. Drug. Discov.* **18**, 1–2 (2019).
61. Ashburn, T. T. & Thor, K. B. Drug repositioning: Identifying and developing new uses for existing drugs. *Nat. Rev. Drug. Discov.* **3**, 673–683 (2004).
62. Veale, C. G. L. & Hoppe, H. C. Screening of the Pathogen Box reveals new starting points for anti-trypanosomal drug discovery. *Medchemcomm* **9**, 2037–2044 (2018).
63. Dandachi, I., Chaddad, A., Hanna, J., Matta, J. & Daoud, Z. Understanding the epidemiology of multi-drug resistant gram-negative bacilli in the middle east using a one health approach. *Front. Microbiol.* **10**, 1941 (2019).
64. Wang, X., *et al.* Identification of *Plasmodium falciparum* mitochondrial malate: Quinone oxidoreductase inhibitors from the pathogen box. *Genes (Basel)*. **10**, 471 (2019).
65. Dans, M. G. *et al.* Screening the Medicines for Malaria Venture Pathogen Box for invasion and egress inhibitors of the blood stage of *Plasmodium falciparum* reveals several inhibitory compounds. *Int. J. Parasitol.* **50**, 235–252 (2020).
66. Spalenka, J., *et al.* Discovery of new inhibitors of toxoplasma gondii via the Pathogen Box. *Antimicrob. Agents Chemother*. **62**, e01640–17 (2018).
67. Mayer, F.L. & Kronstad, J.W. Discovery of a novel antifungal agent in the Pathogen Box. *mSphere* **2**, e00120–17 (2017).
68. Baell, J. B. & Holloway, G. A. New substructure filters for removal of pan assay interference compounds (PAINS) from screening libraries and for their exclusion in bioassays. *J. Med. Chem.* **53**, 2719–2740 (2010).
69. Cowman, A. F., Healer, J., Marapana, D. & Marsh, K. Malaria: Biology and disease. *Cell* **167**, 610–624 (2016).
70. White, N. J. *et al.* Malaria. *Lancet* **383**, 723–735 (2014).
71. Phillips, M. A. *et al.* Malaria. *Nat. Rev. Dis. Primers* **3**, 17050 (2017).
72. Farshi, P. *et al.* Deubiquitinases (DUBs) and DUB inhibitors: A patent review. *Expert Opin. Ther. Pat.* **25**, 1191–1208 (2015).
73. Franco, J. *et al.* A structural comparative approach to identifying novel antimalarial inhibitors. *Comput. Biol. Chem.* **45**, 42–47 (2013).
74. Zhou, P., Zou, J., Tian, F. & Shang, Z. Fluorine bonding how does it work in protein–ligand interactions?. *J. Chem. Inf. Model.* **49**, 2344–2355 (2009).

75. Pasca, M. R. *et al.* Clinical isolates of *Mycobacterium tuberculosis* in four European hospitals are uniformly susceptible to benzothiazinones. *Antimicrob. Agents Chemother.* **54**, 1616–1618 (2010).
76. Gao, C. *et al.* Benzothiazinethione is a potent preclinical candidate for the treatment of drug-resistant tuberculosis. *Sci. Rep.* **6**, 29717 (2016).
77. Vera-Cabrera, L., Campos-Rivera, M. P., Gonzalez-Martinez, N. A., Ocampo-Candiani, J. & Cole, S. T. In vitro activities of the new antitubercular agents PA-824 and BTZ043 against Nocardia brasiliensis. *Antimicrob. Agents Chemother.* **56**, 3984–3985 (2012).
78. Grover, S. *et al.* Benzothiazinones mediate killing of Corynebacterineae by blocking decaprenyl phosphate recycling involved in cell wall biosynthesis. *J. Biol. Chem.* **289**, 6177–6187 (2014).
79. Makarov, V. *et al.* Benzothiazinones kill *Mycobacterium tuberculosis* by blocking arabinan synthesis. *Science* **324**, 801–804 (2009).
80. Gangjee, A., Li, W., Yang, J. & Kisliuk, R. L. Design, synthesis, and biological evaluation of classical and nonclassical 2-amino-4-oxo-5-substituted-6-methylpyrrolo[3,2-d]pyrimidines as dual thymidylate synthase and dihydrofolate reductase inhibitors. *J. Med. Chem.* **51**, 68–76 (2008).
81. Forli, S. *et al.* Computational protein-ligand docking and virtual drug screening with the AutoDock suite. *Nat. Protoc.* **11**, 905–919 (2016).
82. Daina, A., Michielin, O. & Zoete, V. SwissADME: A free web tool to evaluate pharmacokinetics, drug-likeness and medicinal chemistry friendliness of small molecules. *Sci. Rep.* **7**, 42717 (2017).
83. Raza, M., Bharti, H., Singal, A., Nag, A. & Ghosh, P. C. Long circulatory liposomal maduramicin inhibits the growth of *Plasmodium falciparum* blood stages in culture and cures murine models of experimental malaria. *Nanoscale* **10**, 13773–13791 (2018).
84. Lambros, C. & Vanderberg, J.P. Synchronization of *Plasmodium falciparum* erythrocytic stages in culture. *J. Parasitol.* **65**, 418–420 (1979).
85. Smilkstein, M., Sriwilaijaroen, N., Kelly, J. X., Wilairat, P. & Riscoe, M. Simple and inexpensive fluorescence-based technique for high-throughput antimalarial drug screening. *Antimicrob. Agents Chemother.* **48**, 1803–1806 (2004).
86. Terkuile, F., White, N., Holloway, P., Pasvol, G. & Krishna, S. *Plasmodium falciparum*: In vitro studies of the pharmacodynamic properties of drugs used for the treatment of severe malaria. *Exp. Parasitol.* **76**, 85–95 (1993).
87. Pachauri, M., Gupta, E. D. & Ghosh, P. C. Piperine loaded PEG-PLGA nanoparticles: Preparation, characterization and targeted delivery for adjuvant breast cancer chemotherapy. *J. Drug Deliv. Sci. Technol.* **29**, 269–282 (2015).

Acknowledgements

The authors express sincere thanks to the Medicines of Malaria Ventures (MMV) for providing Pathogen Box compounds. We thank Dr. Hidde Ploegh (Boston Children's Hospital, MA) and Dr. Katerina Artavanis-Tsakonas (Department of Pathology, University of Cambridge, UK) for generously sharing the plasmid *pET28a(+)*-PfUCHL3. We also thank Central Instrumentation Facility, University of Delhi, South Campus for providing plate reader and other instrumentation facilities. Our special thanks to the Rotary Blood Bank, Tughlakabad, New Delhi for the generous donation of blood for all our parasite culture studies.

Author contributions

H.B. designed and performed most of the experiments, critically analyzed the results, carried out literature survey and prepared the manuscript. A.S. helped with some experiments and critical analysis of the manuscript. M.S. helped with some in-silico experiments, contributed towards data generation, analysis and manuscript drafting. P.S.C. helped with some experiments and critical analysis of the manuscript. M.R. contributed towards data interpretation and critical review of the manuscript. S.K. provided expert suggestions, shared lab facilities and critically edited the manuscript. A.N. contributed to overall supervision, critical data analysis, critical editing of the manuscript and fund acquisition. All the authors analyzed the results and approved the final version of the manuscript.

Funding

This work was supported by Faculty Research Programme Grant from Institution of Eminence of Delhi University (IoE/FRP/LS/2020/27 and IoE/2021/12/FRP), CSIR EMR Grant, Government of India (37(1682)/17/EMR-II), DBT Grant, Government of India (BT/PR15422/MED/30/1705/2016) to AN and DU-DST (PURSE Grant: RC/2014/7114) and UGC-SAP Grant (F.3.3./2016 DRS II UGC-SAP II), Government of India to AN and SK. Fellowships from CSIR, Government of India to HB,Lady TATA Memorial Trust, India to AS and ICMR, Government of India to MS are thankfully acknowledged.

Competing interests

The authors declare no competing interests.

Additional information

Supplementary Information The online version contains supplementary material available at https://doi.org/10.1038/s41598-021-04619-4.

Correspondence and requests for materials should be addressed to A.N.

Reprints and permissions information is available at www.nature.com/reprints.

Publisher's note Springer Nature remains neutral with regard to jurisdictional claims in published maps and institutional affiliations.